SPECIAL TOPIC — Physical research in liquid crystals

Optical simulation of in-plane-switching blue phase liquid crystal display using the finite-difference time-domain method*

Hu Dou(窦虎)[1], Hongmei Ma(马红梅)[1,2], and Yu-Bao Sun(孙玉宝)[1,2,†]

[1] *Department of Applied Physics, Hebei University of Technology, Tianjin* 300401, *China*

[2] *Tianjin Key Laboratory of Electronic Materials and Devices, Hebei University of Technology, Tianjin* 300130, *China*

(Received 6 May 2016; published online 19 July 2016)

The finite-difference time-domain method is used to simulate the optical characteristics of an in-plane switching blue phase liquid crystal display. Compared with the matrix optic methods and the refractive method, the finite-difference time-domain method, which is used to directly solve Maxwell's equations, can consider the lateral variation of the refractive index and obtain an accurate convergence effect. The simulation results show that e-rays and o-rays bend in different directions when the in-plane switching blue phase liquid crystal display is driven by the operating voltage. The finite-difference time-domain method should be used when the distribution of the liquid crystal in the liquid crystal display has a large lateral change.

Keywords: finite-difference time-domain method, blue phase liquid crystal display, in-plane switching, convergence effect

PACS: 42.79.Kr, 61.30.Cz, 61.30.Mp **DOI:** 10.1088/1674-1056/25/9/094221

1. Introduction

In recent years, blue phase liquid crystal displays[1–3] (BPLCD) have become increasingly attractive because of their features, such as: no need for a surface alignment layer, submillisecond response time, and isotropic dark state for wide viewing angle. The optical simulation of a liquid crystal display (LCD) is usually based on matrix-type solvers. The earliest solver is the simple Jones 2×2 method,[4] this method is only used to calculate the optical properties of normal incident light. The Berreman 4×4 method was proposed to simulate the optical properties of oblique incident light, and it is still a priceless tool to predict the optical properties of liquid crystals.[5] The extended Jones 2×2 method was also proposed to simulate the oblique incident through sampling the Berreman method.[6] In these matrix-type methods, the dielectric tensor of the liquid crystal is assumed to change only along the normal direction of the liquid crystal layer. The liquid crystal layer is first divided into many layers, and then each layer is assumed to be represented by a uniform dielectric tensor. These methods are only used for simple liquid crystal displays (LCDs) without non-uniform distribution of liquid crystal in the horizontal direction. The LCD modes that are used in a large screen LCDs are multi-domain vertical alignment (MVA) and in-plane-switching (IPS). The optical profiles simulated by the extended Jones or Berreman method match to the experimental results, even if the distribution of the liquid crystal is complex in the horizontal direction, but it cannot simulate complex optical phenomenon, such as the convergence effect.[7] In a BPLCD, in-plane electrodes are usually needed to obtain the birefringence in the horizontal direction. The distribution of the refractive index is complex,[8] which needs an accurate method to simulate the optical characteristics. The finite-difference time-domain (FDTD) method directly solves Maxwell's equations and the effect of both the transverse field and the longitudinal field could be taken into account.[9] Therefore, this method can be used to calculate the complex optical profile of the multi-dimensional inhomogeneity of a liquid crystal system. The simulation results compared with those of the matrix-type methods and experiments demonstrate that the FDTD method can give more accurate results.[10–17]

In BPLCD, the BPLC turns into anisotropic from isotropic when an electric field $\boldsymbol{E}$ is applied, and tends to a saturation state. This transition could be described by the extended Kerr formula, and the varied electric field leads to the different birefringence. In IPS-BPLCD, whih is the distribution of refraction index for extraordinary and ordinary light, is non-uniform because of the non-uniform electric field strength induced by the in-plane electrodes. To address the effect of refraction, a refraction model has been proposed to analyze the ray tracing of TE and TM polarizations,[18] which is based on the refraction law and is similar to the light-path tracing

*Project supported by the National Natural Science Foundation of China (Grant Nos. 11304074, 61475042, and 11274088), the Natural Science Foundation of Hebei Province, China (Grant Nos. A2015202320 and GCC2014048), and the Key Subject Construction Project of Hebei Province University, China.

†Corresponding author. E-mail: sun_yubao@163.com

© 2016 Chinese Physical Society and IOP Publishing Ltd

method. Its accuracy depends on the lattice space's shape. In this paper, we calculate the optical properties of IPS-BPCD using the FDTD method.

2. Model and FDTD method

In our simulation, the IPS electrodes' width and gap are set as 5 μm, the wavelength of light is $\lambda = 633$ nm, the grid of the simulation space is called a Yee cell,[9] and the Yee cell is set as $\Delta x = \Delta y = \Delta z = 20$ nm, which is approximately equal to $\lambda/30$. The time step is $\Delta t = 3.81 \times 10^{-17}$ s. The saturated induced birefringence and the saturation electric field of BPLC are $\Delta n_s = 0.09$ and $E_s = 2.2$ V/μm, respectively, the average refractive index is 1.615, and the dielectric constants of the liquid crystal are $\varepsilon_{//} = 112$ and $\varepsilon_{\perp} = 18$. The simulation space is chosen as 20 μm × 0.1 μm × 7.5 μm, corresponding to the thicknesses of the x, y, and z directions of the liquid crystal layer. This means that the thickness of the LC layer is 7.5 μm and the period of the electrodes is 20 μm. The computational space is terminated along the z direction by imposing a perfectly matched layer (PML).[19] In x and y directions, the periodic boundary conditions (PBC) are set to simplify the computational process. Two polarizers' transmissive axial directions are oriented at ±45° with respect to the IPS electrode, respectively. A schematic of the structure of the liquid crystal layer is shown in Fig. 1.

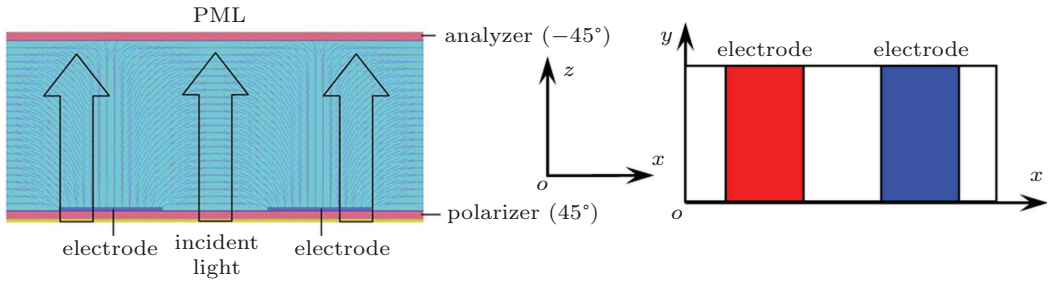


Fig. 1. (color online) A schematic of the structure and coordinate system of IPS-BPLC.

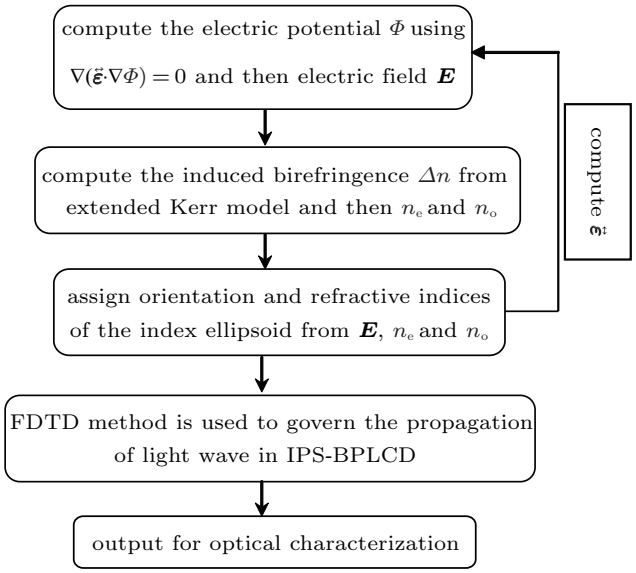


Fig. 2. Flowchart of the IPS-BPLCD model based on the FDTD method.

To calculate the optical characterization of IPS- PLCD, the flowchart in Fig. 2 is used to model the IPS-BPLCD. First, we compute the electric potential distribution Φ by solving the Poisson equation $\nabla(\overleftrightarrow{\varepsilon} \cdot \nabla\Phi) = 0$, and then the electric field's distribution $\boldsymbol{E}$ in the BPLC layer. $\overleftrightarrow{\varepsilon}$ is the effective dielectric tensor of the BPLC material under a low frequency electric field, which is related to the electric field's distribution and strength. This step can be done with commercial software (TechWiz LCD). To simulate with the FDTD method, we divide the cell into Yee cells, as shown in the previous paragraph. Second, with the electric field, we calculate the induced birefringence distribution from the extended Kerr equation[20]

$$\Delta n_{\text{ind}} = \Delta n_s \left(1 - \exp\left[-(E/E_s)^2\right]\right), \tag{1}$$

where Δn_s and E_s stand for the saturated induced birefringence and the saturation electric field, respectively. The refractive index's distributions can then be obtained as

$$n_e = n_i + \frac{2}{3}\Delta n_{\text{ind}}, \quad n_o = n_i - \frac{1}{3}\Delta n_{\text{ind}}, \tag{2}$$

where n_e is the local optic axis direction along the $\boldsymbol{E}$ vector, and n_o is perpendicular to the $\boldsymbol{E}$ vector. The induced birefringence and the effective dielectric tensor are dependent on the electric field strength, so a few-cycle calculations are required to obtain the stable condition before moving to the next step. The FDTD method is a powerful approach to solve Maxwell's time-dependent curl equations, which govern the propagation of light. For nonmagnetic anisotropic media, discrete expressions of electric and magnetic fields in Maxwell's equations can be approximated using the central difference scheme based on the Yee grid, as follows:[9]

$$E^n = E^{n-1} + \frac{\Delta t}{\varepsilon_0}\widetilde{\varepsilon}^{-1} \cdot \nabla \times H^{n-1/2}, \tag{3}$$

$$H^{n+1/2} = E^{n-1/2} - \frac{\Delta t}{\mu_0} \cdot \nabla \times E^n. \tag{4}$$

Here, n represents the time points, Δt is the time step, and $\widetilde{\varepsilon}$ is the spatially varying relative permittivity tensor in uniaxial LC medium and is written in the xyz coordinate system as

$$\widetilde{\varepsilon} = \begin{bmatrix} \varepsilon_{xx} & \varepsilon_{xy} & \varepsilon_{xz} \\ \varepsilon_{yx} & \varepsilon_{yy} & \varepsilon_{yz} \\ \varepsilon_{zx} & \varepsilon_{zy} & \varepsilon_{zz} \end{bmatrix}, \tag{5}$$

with

$$\begin{aligned}
\varepsilon_{xx} &= n_{\mathrm{o}}^2 + (n_{\mathrm{e}}^2 - n_{\mathrm{o}}^2)\cos^2\theta\cos^2\phi, \\
\varepsilon_{xy} &= \varepsilon_{yx} = (n_{\mathrm{e}}^2 - n_{\mathrm{o}}^2)\cos^2\theta\sin\phi\cos\phi, \\
\varepsilon_{xz} &= \varepsilon_{zx} = (n_{\mathrm{e}}^2 - n_{\mathrm{o}}^2)\cos\theta\sin\theta\cos\phi, \\
\varepsilon_{yy} &= n_{\mathrm{o}}^2 + (n_{\mathrm{e}}^2 - n_{\mathrm{o}}^2)\cos^2\theta\sin^2\phi, \\
\varepsilon_{yz} &= \varepsilon_{zy} = (n_{\mathrm{e}}^2 - n_{\mathrm{o}}^2)\cos\theta\sin\theta\sin\phi, \\
\varepsilon_{zz} &= n_{\mathrm{o}}^2 + (n_{\mathrm{e}}^2 - n_{\mathrm{o}}^2)\sin^2\theta,
\end{aligned}$$

where n_{e} and n_{o} are obtained from the above step, θ is the tilt angle between the local optic axis direction and the surface of the substrate (xy-plane), and ϕ is the azimuthal angle between the projection of the local optic axis on the xy plane and the x axis. Once $\widetilde{\varepsilon}$ is obtained at every Yee grid point within the computation space, the sequence of light propagation in the structure can proceed, which is ruled by the time updating algorithm from Maxwell's equations. At last, the optical characterization is obtained.

3. Simulation results

Voltage dependent transmittance curves of IPS-BPLCD simulated by different methods are shown in Fig. 3. The black line represents the Jones matrix method, the black square line is for the FDTD method, the blue solid line represents the refractive method, and the red solid line represents the experimental results. The Ge's model (Jones method) is lower than the experimental results, the refractive method fits the experimental results, and the FDTD method fits the experimental result at the low voltage and is different from the experimental results. To find the reasonable method, we calculate the transmittance of different position for the cell with the maximum transmittance, as shown in Fig. 4. From these figures, we can see that the transmittance above the electrodes is very small using the Jones and FDTD methods but is relatively higher using the refractive method. The maximum transmittance in Fig. 4(a) is 1.0 because there is no light convergence effect in the Jones method, and is larger than 1.0 in Figs. 4(b) and 4(c). By carefully investigating the transmittance above the electrodes in the refractive method, a discontinuous change can be seen, which means that this method has some approximation and so it may not give an accurate result. The continuous change in the FDTD method means that it can give a reasonable result. The difference between the simulation and the experiment may come from the difference of the parameters in the simulation and the real cell.

After light penetrates through the LC cell, the convergence effect can be seen. Set the PML at four positions $z = 0$ μm, $z = 1$ μm, $z = 2$ μm, and $z = 3.2$ μm, where z is distance from the top surface of the cell, and the thickness of the glass and polarizer is ignored. The transmittance versus x-position for the operating voltage is shown in Fig. 5. The peak transmittance increases and moves to the center of the electrode gaps. The convergence effect can be seen because of the symmetric electric field distribution induced by the IPS electrodes.

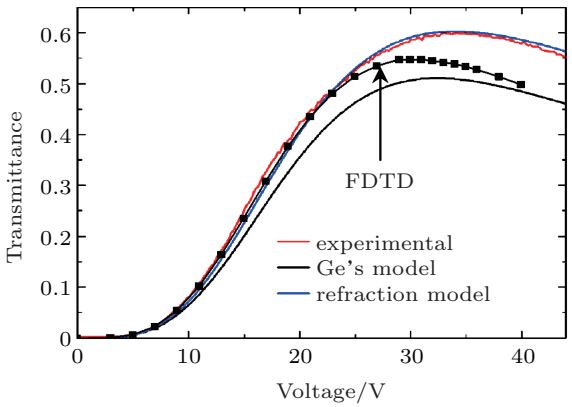


Fig. 3. (color online) Voltage dependent transmittance curves of IPS-BPLCD obtained by different simulation methods. The result of refractive method and experimental results are from Ref. [18].

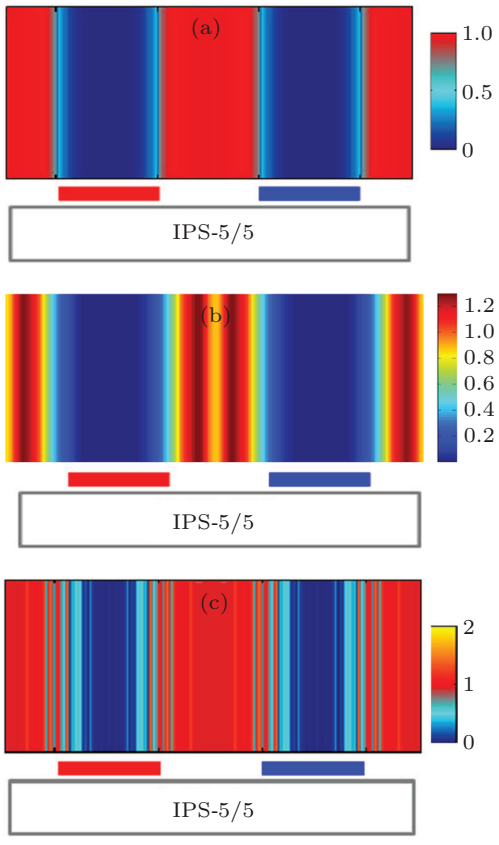


Fig. 4. (color online) Transmittance for the cell driven by the operating voltage using (a) Jones method, (b) FDTD method, and (c) refractive method.[18]

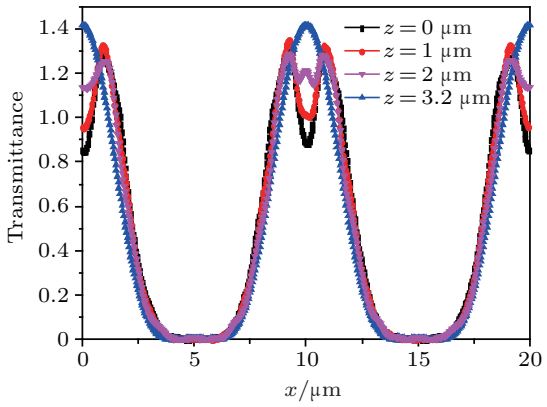


Fig. 5. (color online) Transmittance vs x-position for $z = 0$ μm, $z = 1$ μm, $z = 2$ μm, and $z = 3.2$ μm.

The angle between the polarizer and the x axis is 45°. Therefore, the polarization light could be considered as two same strength linear polarized lights when the light passes through BPLC layer because the electric field changes in the xoz plane. The two linear polarization light's directions are along x and y axes, corresponding to the e-ray and o-ray. For the o-ray, the refractive index of the BPLC layer is n_o, which is the ordinary refractive index of BPLC, it is noteworthy that n_o is not a constant because it relates to the electric field strength. For the e-ray, the effective refractive index of the BPLC layer is

$$n'_e = \frac{n_e n_o}{\sqrt{n_o^2 + (n_e^2 - n_o^2)\sin^2(\theta)}}, \tag{6}$$

where n_e is the extraordinary refractive index induced by the electric field, and θ is the tilt angle of the electric field direction with respect to the x axis. The distribution of n'_e and n_o can be calculated for the cell under the operating voltage for the maximum transmittance, as shown in Fig. 6.

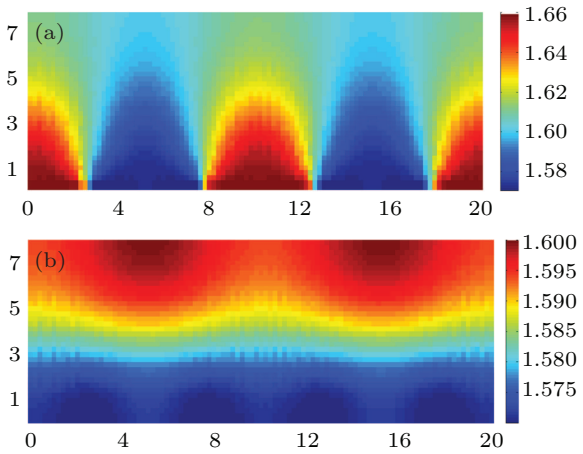


Fig. 6. (color online) Distributions of effective refractive indexes of (a) e-ray and (b) o-ray.

Considering the electrode structure and the Kerr effect of BPLC, we find that the variation of the refractive index occurs in the xoz plane. As shown in Fig. 6, the effective refractive indexes for o-ray and e-ray vary with the position, the largest refractive index of e-ray appears in the gap of the electrodes, and the least refractive index of ordinary light appears at the edges of the electrodes. The distribution shows that the change of the effective refractive index of the e-ray mainly occurs along the x-axis and that of the o-ray mainly occurs along the z-axis.

As shown in Fig. 7, short pulse e-rays and o-rays are used to simulate their variations in the BPLC layer. The wave surface of the light is distorted because the propagation velocity of the e-ray is different from the variety of the effective refractive index. From Fig. 6(a), the effective refractive index of the e-ray at the center of the electrodes is lager than that at the edges of the electrodes, the BPLC layer above the electrodes' gap behaves just like a convex lens, converging the e-ray to the center of the electrode gaps. The red circles in Fig. 7(a) show the convergence zones. This convergence effect allows some light above the electrodes to bend to the electrodes' gaps, as shown in Fig. 4(b), which can improve the transmission. From Fig. 7(b), the propagation velocities of the o-ray are almost the same because the lateral variation of the effective refractive index of the o-ray is very small, so little convergence effect occurs, which is marked by the red circles in Fig. 7(b). The convergence zone of the o-ray is contrary to that of the e-ray but is negligible because the difference of the refractive index for an e-ray and an o-ray above the electrodes is nearly zero.

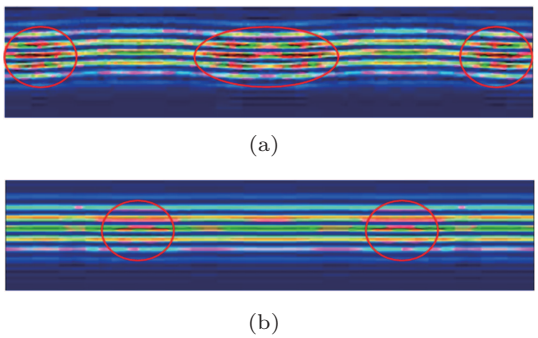


Fig. 7. (color online) Wave surface and strength of short pulse (a) e-rays and (b) o-rays penetrating through IPS-BPLCD and driven by the operating voltage.

A short pulse light is used to simulate the transmittance when it is propagating in IPS-BPLCD driven by the operating voltage. The results at different times are shown in Fig. 8. The under and upper milky white rectangles are the polarizer and the analyzer, respectively. The plane wave light enters the polarizer, the linear polarization light is generated with the same wave surface and strength, as shown in Fig. 8(a). From Fig. 6 it can be seen that the birefringence above the electrodes is very small, so the wave surface above the electrodes does not change, except at the edges of the electrodes. Between the electrodes, the birefringence effect makes the wave surface lower than that above the electrodes, and the wave surface is

curved, as shown in Figs. 8(b) and 8(c). As the light arrives at the analyzer, the light above the electrodes is absorbed and reflected because the polarization direction of the light wave is perpendicular to the axis of the analyzer. The light between the electrodes is wholly transmitted without reflection because the polarization direction of the light wave is parallel to the axis of the analyzer, as shown in Fig. 8(d). After the light transmits out of the LCD, the traveled light has little difference at different position because of the convergence effect, so the convergence curves in Fig. 5 can be obtained.

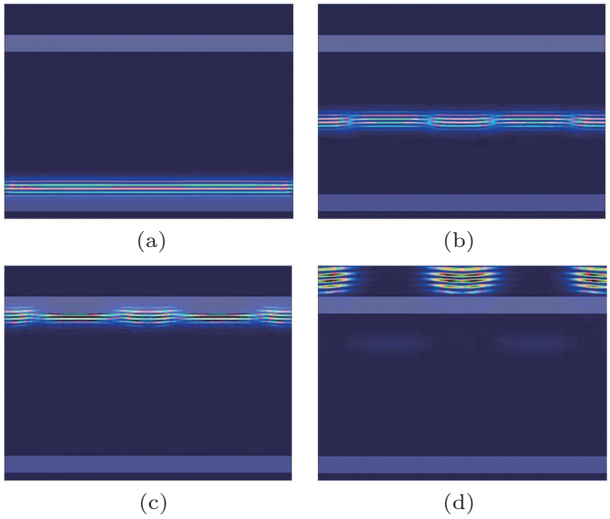


Fig. 8. (color online) A short pulse light transmits through IPS-BPLCD driven by the operating voltage. Panels (a)–(d) show the light wave at different times.

4. Conclusion

The FDTD method has been used to simulate the optical characteristics of IPS-BPLCD. Compared with the Jones matrix method and the refractive method, the FDTD method has the most rigorous theory. When light passes through the IPS-BPLC cell, a convergence effect can be calculated. The simulation result indicates that the convergence zones are reversed for o-rays and e-rays, but the convergence effect of the o-rays is infinitesimally small and can be ignored. The convergence effect is mainly seen for e-rays in IPS-BPLCD, which leads a part of the light to bend to the electrode gaps from the edges of the electrodes and improves the transmittance of IPS-LCD.

References

[1] Choi S W, Yamamoto S I, Haseba Y, Higuchi H and Kikuchi H 2008 *Appl. Phys. Lett.* **92** 043119
[2] Chen K M, Gauza S, Xianyu H and Wu S T 2010 *J. Disp. Technol.* **6** 49
[3] Zhao Y, Sun Y, Li Y and Ma H 2014 *Liq. Cryst.* **41** 1583
[4] Jones R C 1941 *J. Opt. Soc. Am.* **31** 488
[5] Berreman D W 1972 *J. Opt. Soc. Am.* **62** 502
[6] Lien A 1990 *Appl. Phys. Lett.* **57** 2767
[7] Yang D K and Wu S T 2015 *Fundamentals of Liquid Crystal Devices* (Chichester: John Wiley & Sons, Ltd)
[8] Rao L, Yan J, Wu S T, Yamomoto S and Haseba Y 2011 *Appl. Phys. Lett.* **98** 081109
[9] Yee K S 1966 *IEEE Trans. Antennas Propag.* **14** 302
[10] Kriezis E E and Elston S J 1999 *Opt. Commun.* **165** 99
[11] Kriezis E E and Elston S J 2000 *Opt. Commun.* **177** 69
[12] Hwang D K and Rey A D 2005 *Appl. Optics* **44** 4513
[13] Prokopidis K P, Zografopoulos D C and Kriezis E E 2013 *J. Opt. Soc. Am. B* **30** 2722
[14] Ogawa Y, Fukuda J I, Yoshida H and Ozaki M 2013 *Opt. Lett.* **38** 3380
[15] Dou H, Yu Y, Ma H and Sun Y 2015 *Chin. J. Liq. Cryst. Disp.* **30** 16
[16] Dou H, Yu Y, Ma H and Sun Y 2015 *Chin. J. Liq. Cryst. Disp.* **30** 381
[17] Dou H, Ma H and Sun Y 2015 *Acta Phys. Sin.* **64** 126101 (in Chinese)
[18] Xu D, Chen Y, Liu Y and Wu S T 2013 *Opt. Express* **21** 24721
[19] Berenger J P 1994 *J. Comput. Phys.* **114** 185
[20] Yan J, Cheng H C, Gauza S, Li Y, Jiao M, Rao L and Wu S T 2010 *Appl. Phys. Lett.* **96** 071105